STABITITY ANALYSIS OF A FLEXIBE ROTOR SUPPORTED BY PASSIVELY OR ACTIVELY LUBRICATED HYBRID MULTIRECESS JOURNAL BEARING

Flávio Yukio Watanabe
FEAU – Faculty of Engineering, Architecture and Urbanism
UNIMEP – Methodist University of Piracicaba
18450-000, Sta. Bárbara d'Oeste – SP – Brazil
fywatana@unimep.br

Ilmar Ferreira Santos
MEK – Department of Engineering
DTU – Technical University of Denmark
2800, Lyngby – Denmark
ifs@mek.dtu.dk

Abstract. Fluid film forces are generated in multirecess journal bearings by two types of lubrication mechanism: the hydrostatic lubrication in the bearing recesses and hydrodynamic lubrication in the bearing lands, when operating in rotation. The combination of both lubrication mechanism leads to hybrid journal bearings (HJB). When part of hydrostatic pressure is also dynamically modified by means of hydraulic control systems, one refers to the active lubrication, resulting in the active hybrid journal bearing (AHJB). The AHJB is mathematically modeled based on the Reynolds' equations in land regions and a set of modified continuity equations for the lubricant flow in the bearing recesses, coupled to equations describing pressure and flow in the servovalves. The solution of such a set o equations allows the determination of fluid film stiffness and damping coefficients of the hybrid and/or active lubricated bearing. Such coefficients are a function of design and operational parameters, characterized by the Sommerfeld number as well by the gains of the feedback control system. The main contribution of the present theoretical work is to analyze the stability characteristics of a flexible rotor-bearing system by using passively and actively lubricated hybrid journal bearing. The dynamic of a flexible rotor is modeled by using finite element method and, after coupling the bearing dynamic coefficients to the rotor model, the feedback control law is defined and a suitable set of control gains is calculated for the active lubrication, leading to a rotor with a wider and more safety operational frequency range

Keywords: Hybrid Bearing, Active Lubrication, Vibration Control, Stability

1. Introduction

Aiming for the vibration reduction in rotating machines to safety levels, new mechanisms for dissipating vibration energy have been developed, like seal dampers (Vance and Li, 1996), squeeze-film dampers (San Andrés and Lubell, 1998), hybrid squeeze-film dampers (El-Shafei and Halthout, 1995), hydraulic active chamber systems (Ulbrich and Althauss, 1989; Althaus *et al*., 1993; Santos, 1995), variable impedance hydrodynamic journal bearings (Goodwin *et al*., 1989), actively lubricated tilting-pad bearings (Santos, 1994; Santos and Russo, 1998; Santos e Nicoletti, 1999; Santos and Scalabrin, 2000), active-controlled hydrostatic bearings (Bently *et al*., 1999), magnetized journal bearings lubricated with Ferro fluids (Osman *et al*., 2001), and actively lubricated hybrid multirecess journal bearings (Santos and Watanabe, 2003 and 2004).

Recent theoretical (Santos, 1994; Santos and Russo, 1998; Santos and Nicoletti, 2001) and experimental (Santos and Scalabrin, 2000; Santos *et al*., 2001) investigations related to active lubrication have been shown the feasibility of attenuating rotor vibrations in test rigs with rigid rotors. The use of active lubrication in tilting-pad journal bearings (TPJB) has the strong advantage of resulting to bearings with negligible fluid film cross-coupling effects between orthogonal directions. However, this kind of active strategy can also be applied to hydrostatic or hybrid bearings (Bently *et al*., 2000; Santos and Watanabe, 2003 and 2004), and to multi-lobed bearings (Santos *et al*., 2001).

The main contribution of the present theoretical work is to analyze the feasibility of applying multirecesses hybrid journal bearings (HJB) with active lubrication to a flexible rotor, aiming the attenuation of rotor-bearing system vibrations, through the active modifications of the stiffness and damping bearings coefficients. The hybrid journal bearing mathematical model presented by Ghosh *et al*. (1989) and Guha *et al*. (1989) is extended by including the dynamics of servo control system, as presented by Santos and Russo (1998). By dynamically controlling the hydrostatic pressure and flow into opposed bearing recesses with help of servo-hydraulic control systems, significant modification of fluid film flow and forces can be achieved. A multirecesses hybrid journal bearing with active lubrication is termed active hybrid journal bearing (AHJB). The AHJB static and dynamic coefficients are numerically calculated by solving the complete set of continuous equation in recesses regions and Reynolds' Equation in land regions, as a function of Sommerfeld number, perturbation frequency, servovalve dynamic characteristics and feedback control gains. These

bearing coefficients, with and without active lubrication, are employed to analyze the vibration reduction influence in a flexible rotor. The rotor flexibility is considered in the analysis by using finite elements modeling technique.

2. Active Hybrid Journal Bearing - AHJB

The AHJB under investigation has four recesses, aligned in pairs in the horizontal (Y) and vertical (X) directions and numbered as shown in Fig. 1a. The conventional passive bearing operation is warranted by fluid injection into the recesses through capillary restrictors, at a constant pressure supply P_{s0}. Additionally, for active dynamic control of the fluid pressure and compensation of cross-coupling effects, the flow is injected into the opposed bearing recesses pairs, each one of them are connected to servo control systems. Electrohydraulic servovalves, journal displacement and/or velocity transducers and PD feedback controllers constitute the servo control system. The servovalves are controlled by electrical voltage signals, U_X and U_Y, generated by the combination of journal dynamic displacement and velocity measurement signals in X and Y directions. The main geometric characteristics of a four recesses hybrid journal bearing, nomenclature and coordinate systems are represented in Fig. 1.
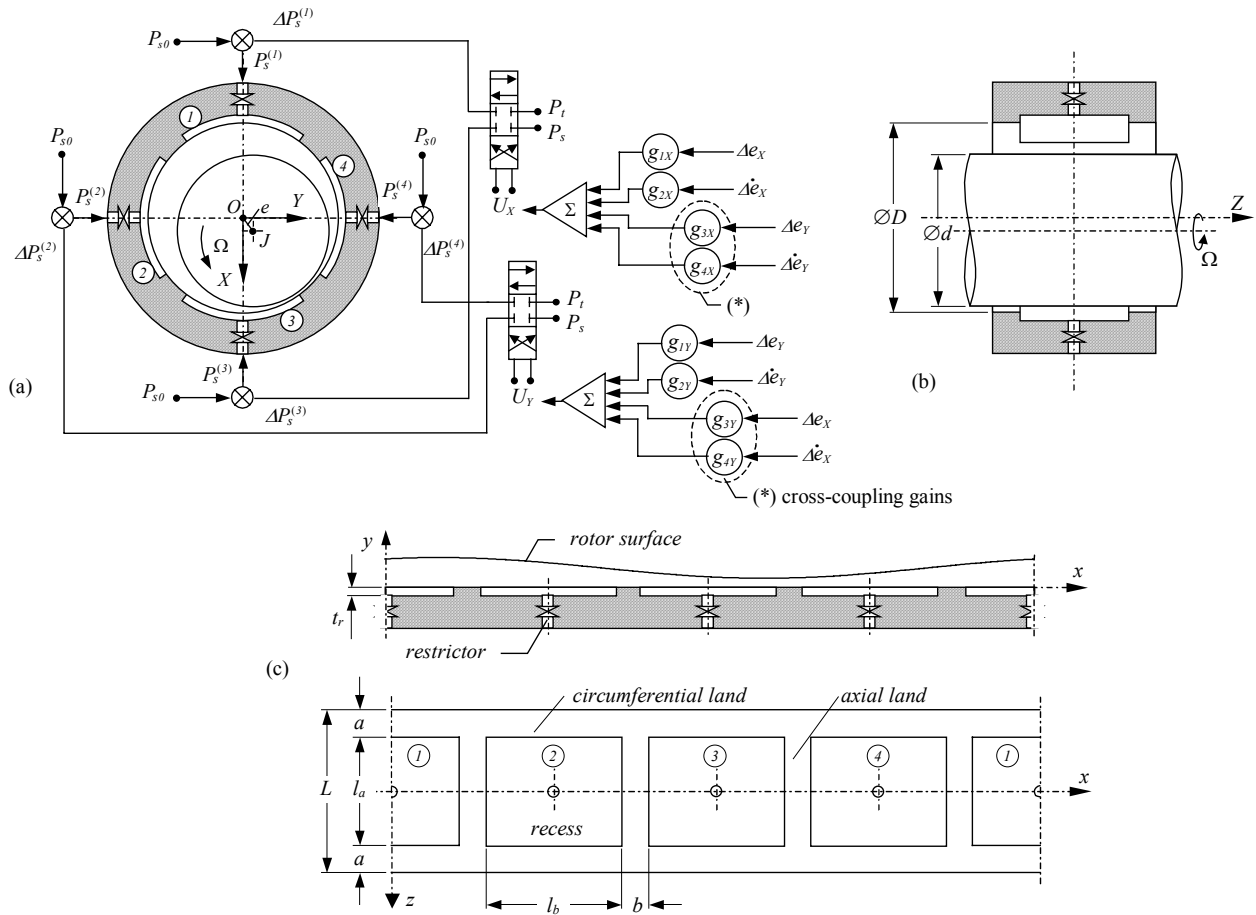
Figure 1. Active Hybrid Journal Bearing – geometric characteristics and operational principle

2.1. AHJB Mathematical Modeling

The mathematical model of the HJB is obtained basically by using the Reynolds' equation in the land surfaces and the flow continuity equation in the bearing recesses, as presented by Santos and Watanabe (2003). The modeling technique used is the small perturbation method applied to the journal steady state equilibrium position (Lund and Thomsen, 1978, and by Ghosh et al., 1989). Within the bearing radial clearance c, the static eccentricity and attitude angle are defined by e_0 and φ_0, respectively, and the journal dynamic perturbations are defined by the real part of the harmonic functions given by $e_1^* e^{i\omega t}$ and $\varphi_1^* e^{i\omega t}$, where, ω is the perturbation frequency, t is the time, and e_1^* and φ_1^* are the perturbations amplitudes. The resulting dimensionless fluid film thickness $\bar{h} = h/c$ is defined as a function of the dimensionless eccentricity $\varepsilon = e/c$, attitude angle components, the angular coordinate $\theta = x/R$, and the dimensionless time $\tau = \omega t$.

$$\begin{cases} \bar{h} = \bar{h}_0 + \varepsilon_1^* e^{i\tau} \cos\theta + \varepsilon_0 \varphi_1^* e^{i\tau} \sin\theta \\ \bar{h}_0 = 1 + \varepsilon_0 \cos\theta \end{cases} \tag{1}$$

Considering the small perturbation characteristics, the dimensionless fluid film pressure $\overline{P} = P/P_{s0}$ may be described similarly to dimensionless film thickness $\overline{h}$, defined Eq. (1), as follows

$$\overline{P} = \overline{P}_0 + \varepsilon_i^* e^{i\tau} \overline{P}_1 + \varepsilon_0 \varphi_i^* e^{i\tau} \overline{P}_2 \tag{2}$$

The fluid film behavior in the land surfaces of a finite bearing is described by the three dimensionless Reynolds' equations, given in Eq. (3-5), deduced by using the Navier-Stokes, continuity equations and Eq. (1-2), considering a isoviscous incompressible fluid, in laminar flow and including the hydrodynamic and squeeze effects.

$$\frac{\partial}{\partial \theta}\left(\overline{h}_0^{\,3}\frac{\partial \overline{P}_0}{\partial \theta}\right) + \left(\frac{D}{L}\right)^2 \frac{\partial}{\partial \overline{z}}\left(\overline{h}_0^{\,3}\frac{\partial \overline{P}_0}{\partial \overline{z}}\right) = \Lambda \frac{\partial \overline{h}_0}{\partial \theta} \tag{3}$$

$$\frac{\partial}{\partial \theta}\left(\overline{h}_0^{\,3}\frac{\partial \overline{P}_1}{\partial \theta}\right) + \frac{\partial}{\partial \theta}\left(3\overline{h}_0^{\,2}\cos\theta\frac{\partial \overline{P}_0}{\partial \theta}\right) + \left(\frac{D}{L}\right)^2 \frac{\partial}{\partial \overline{z}}\left(\overline{h}_0^{\,3}\frac{\partial \overline{P}_1}{\partial \overline{z}}\right) + \left(\frac{D}{L}\right)^2 \frac{\partial}{\partial \overline{z}}\left(3\overline{h}_0^{\,2}\cos\theta\frac{\partial \overline{P}_0}{\partial \overline{z}}\right) = -\Lambda\sin\theta + i\Psi\cos\theta \tag{4}$$

$$\frac{\partial}{\partial \theta}\left(\overline{h}_0^{\,3}\frac{\partial \overline{P}_2}{\partial \theta}\right) + \frac{\partial}{\partial \theta}\left(3\overline{h}_0^{\,2}\cos\theta\frac{\partial \overline{P}_0}{\partial \theta}\right) + \left(\frac{D}{L}\right)^2 \frac{\partial}{\partial \overline{z}}\left(\overline{h}_0^{\,3}\frac{\partial \overline{P}_2}{\partial \overline{z}}\right) + \left(\frac{D}{L}\right)^2 \frac{\partial}{\partial \overline{z}}\left(3\overline{h}_0^{\,2}\cos\theta\frac{\partial \overline{P}_0}{\partial \overline{z}}\right) = \Lambda\cos\theta + i\Psi\sin\theta \tag{5}$$

where,

$\overline{z} = 2z/L$ dimensionless z coordinate
$\Lambda = 6\mu\Omega/P_{s0}\,(c/R)^2$ angular velocity parameter
$\Psi = 12\mu\omega/P_{s0}\,(c/R)^2$ squeeze or perturbation frequency parameter

Equations (3-5) are solved by using the *finite difference method* with the boundary condition listed below for $k=0,1,2$

(a) $\overline{P}_0(\theta,\overline{z}) = 0$, in the regions of cavitations   (b) $\overline{P}_k = \overline{P}_r^{(n)}$, fluid pressure at the *n-th* recess
(c) $\overline{P}_k(\theta,+1) = \overline{P}_k(\theta,-1) = 0$, for symmetry   (d) $\overline{P}_k(\theta,\overline{z}) = \overline{P}_k(\theta+2\pi,\overline{z})$, for periodicity
(e) $\dfrac{\partial \overline{P}_k}{\partial \overline{z}}(\theta,0) = 0$, for symmetry

The fluid pressures in the recesses are obtained by applying the continuity equation, considering fluid hydrodynamic, hydrostatic, squeeze and compressibility effects. The recess fluid pressures $\overline{P}_r^{(n)}$, in the *n-th* recess, is defined similarly to the fluid film pressure $\overline{P}$ as follows

$$\overline{P}_r^{(n)} = \overline{P}_{r0}^{(n)} + \varepsilon_i^* \overline{P}_{r1}^{(n)} e^{i\tau} + \varepsilon_0 \varphi_i^* \overline{P}_{r2}^{(n)} e^{i\tau} \tag{6}$$

Defining the dimensionless flow $\overline{Q}$ as follows, $\overline{Q} = 12\mu Q/c^3 P_{s0}$, and applying the continuity equation to all recesses, results to the following vector equation

$$\overline{\boldsymbol{q}}_s = \overline{\boldsymbol{Q}}_r\,\overline{\boldsymbol{p}}_r + \Phi\Delta\overline{\boldsymbol{h}} + \Theta\frac{\partial \overline{\boldsymbol{h}}_r}{\partial \tau} + \Pi\overline{\boldsymbol{V}}_e\frac{\partial \overline{\boldsymbol{p}}_r}{\partial \tau} \tag{7}$$

where,

$\overline{\boldsymbol{Q}}_r$ recess flow matrix
$\overline{\boldsymbol{V}}_e$ effective recess volume matrix
$\overline{\boldsymbol{q}}_s = \left\{\overline{Q}_s^{(1)} \quad \overline{Q}_s^{(2)} \quad \overline{Q}_s^{(3)} \quad \overline{Q}_s^{(4)}\right\}'$ fluid flow vector injected into the recesses
$\overline{\boldsymbol{p}}_r = \left\{\overline{P}_r^{(1)} \quad \overline{P}_r^{(2)} \quad \overline{P}_r^{(3)} \quad \overline{P}_r^{(4)}\right\}'$ recess pressure vector
$\overline{\boldsymbol{h}}_r = \left\{\overline{h}_r^{(1)} \quad \overline{h}_r^{(2)} \quad \overline{h}_r^{(3)} \quad \overline{h}_r^{(4)}\right\}'$ film thickness vector at the center recesses
$\Delta\overline{\boldsymbol{h}} = \left\{(\overline{h}_l^{(1)}-\overline{h}_l^{(4)}) \quad (\overline{h}_l^{(2)}-\overline{h}_l^{(1)}) \quad (\overline{h}_l^{(3)}-\overline{h}_l^{(2)}) \quad (\overline{h}_l^{(4)}-\overline{h}_l^{(3)})\right\}'$
$\overline{h}_l^{(n)}$ film thickness between *n-th* and *(n+1)-th* recesses
$\Phi = 6\mu UL_e/c^2 P_{s0}$ recess velocity parameter
$\Theta = 12\mu\omega DL_e \sin(\pi/4)/c^2 P_{s0}$ recess squeeze parameter
$\Pi = 12\mu\omega\kappa/c^3$ recess compressibility parameter

The fluid flow $\overline{q}_s$, injected into the bearing recesses, is resultant of the combination of the conventional lubrication supply and the active lubrication systems, whose main components are the servovalves and the type adopted is a two-stage, four-way, critical center or zero-lapped spool electrohydraulic servovalve. In a typical critical center servovalve, the output spool position is proportional to electrical signal applied to torque motor coils. Movement of the spool opens an orifice from the constant supply pressure P_s to one servovalve port and an identical orifice connects the other servovalve port to the return line to reservoir at pressure P_t.

The dynamics of the fluid flow through an unloaded servovalve can be described by a second order differential equation (Merrit, 1967). The coefficients of such equation, eigenfrequency ω_v, damping factor ζ_v and gain K_v, are obtained from servovalve manufacturers (Neal, 1974 and Edelmann, 1986). Each servovalve, working in orthogonal directions X and Y, is described mathematically as a function of the servovalve dynamic coefficients, the unloaded fluid flows Q_{vX} and Q_{vY} and the input electrical voltage signals U_X and U_Y by

$$\begin{cases} \ddot{Q}_{vX} + 2\zeta_v\omega_v\dot{Q}_{vX} + \omega_v^2 Q_{vX} = \omega_v^2 K_v U_X \\ \ddot{Q}_{vY} + 2\zeta_v\omega_v\dot{Q}_{vY} + \omega_v^2 Q_{vY} = \omega_v^2 K_v U_Y \end{cases} \tag{8}$$

The input signals U_X and U_Y are generated as a linear combination of journal dynamic displacement and velocity sensors signals, and can be expressed as

$$\begin{cases} U_X = g_{1X}\Delta e_X + g_{2X}\Delta\dot{e}_X + g_{3X}\Delta e_Y + g_{4X}\Delta\dot{e}_Y \\ U_Y = g_{1Y}\Delta e_Y + g_{2Y}\Delta\dot{e}_Y + g_{3Y}\Delta e_X + g_{4Y}\Delta\dot{e}_X \end{cases} \tag{9}$$

where,

$\Delta e_X = e_X^* e^{i\omega t}$, $\Delta e_Y = e_Y^* e^{i\omega t}$ journal dynamic displacements in X and Y directions, respectively

$\Delta\dot{e}_X = i\omega\Delta e_X$, $\Delta\dot{e}_Y = i\omega\Delta e_Y$ journal velocities in X and Y directions, respectively

$e_X^* = e_I^* \cos\varphi_0 - e_0\varphi_I^* \sin\varphi_0$, $e_Y^* = e_I^* \sin\varphi_0 + e_0\varphi_I^* \cos\varphi$

$g_{1X}, g_{2X}, g_{3X}, g_{4X}, g_{1Y}, g_{2Y}, g_{3Y}, g_{4Y}$ gain coefficients

As shown in Fig. 1a, the servovalve connected to recesses *1* and *3* is responsible for controlling the journal movement in *X* direction, and the other servovalve connected to recesses *2* and *4* is responsible for controlling the journal movement in *Y* direction. For simplicity, the analysis is led only in Y direction.

The unloaded servovalve flow Q_{vY} can be expressed by $Q_{vY} = Q_{vY}^* e^{i(\omega t + \varphi_Y)}$, once it is proportional to the harmonic journal eccentricity. Assuming that the gain coefficients are related as follows: $g_{3Y} = k_g g_{1Y}$ and $g_{4Y} = k_g g_{2Y}$, one can deduce the Q_{vY} expression from Eq. (8), in dimensionless form

$$\overline{Q}_{vY} = (\varepsilon_Y^* + k_g \varepsilon_X^*)G_Y e^{i(\omega t + \varphi_Y)} \tag{10}$$

where,

$$G_Y = \frac{12\mu\omega_v^2 K_v}{c^2 P_{s0}}\sqrt{\frac{g_{1Y}^2 + \omega^2 g_{2Y}^2}{(\omega_v^2 - \omega^2)^2 + (2\zeta_v\omega_v\omega)^2}} \quad \text{and} \quad \varphi_Y = tg^{-1}\left\{\frac{-2\zeta_v\omega_v\omega g_{1Y} + \omega(\omega_v^2 - \omega^2)g_{2Y}}{(\omega_v^2 - \omega^2)g_{1Y} + 2\zeta_v\omega_v\omega^2 g_{2Y}}\right\}$$

The active fluid flow injected in *Y* direction Q_Y may be given in the following dimensionless form

$$\overline{Q}_Y = \overline{Q}_{vY} - \overline{K}_{PQ}\overline{P}_{LY} \tag{11}$$

where,

$K_{PQ} = (\partial Q_Y / \partial P_{LY})_{op}$ servovalve flow-pressure coefficient (*op* – operation point)

$\overline{K}_{PQ} = 12\mu K_{PQ}/c^3$ dimensionless servovalve flow-pressure coefficient

$\overline{P}_{LY} = P_{LY}/P_{s0} = \overline{P}_s^{(2)} - \overline{P}_s^{(4)} \equiv \Delta\overline{P}_s^{(2)} - \Delta\overline{P}_s^{(4)}$ dimensionless load pressure in Y direction

$\Delta P_s^{(2)}$, $\Delta P_s^{(4)}$ dynamic supply pressures in recesses 2 and 4, respectively

The coefficients K_v and K_{PQ} may be experimentally determined as shown by Merrit (1967), and usually are given by servovalve manufacturers. Equation (11) is valid only in a small range of the nominal input signal, usually ±5%. It is important to mention that the gains g_1 and g_2 have to be chosen respecting the linear range of the servovalve dynamics, i.e. the maximum amplitude of the control voltage (servovalve input signal). Mathematically, it means that U_X and U_Y, given by Eq.(9), have to be in the range of ±5% of the nominal voltage. Such an analysis can only be

done knowing the vibration amplitudes of the rotor-bearing system. Generally speaking, the bigger the rotor amplitudes are, the smaller the coefficients g_1 and g_2 can be. The higher the perturbation frequencies ω are, the smaller the coefficient g_2 can be.

Coupling the HJB and servo control system models, results in the complete mathematical model of AHJB (Santos and Watanabe, 2003), and the total fluid flow injected into the bearing recesses are determined as follows

$$\overline{q}_s = \overline{q}_{s0} + (\delta_c\,\overline{p}_{r1} + \overline{g}_{s1})\,\varepsilon_1^*e^{i\tau} + (\delta_c\,\overline{p}_{r2} + \overline{g}_{s2})\,\varepsilon_0\varphi_1^*e^{i\tau} \tag{12}$$

where, $\overline{q}_{s0}$, $\overline{p}_{r1}$ and $\overline{p}_{r2}$ are defined similarly to $\overline{q}_s$ and $\overline{p}_r$, and $\overline{g}_{s1}$ and $\overline{g}_{s2}$ are injection vectors related to the bearing active lubrication system.

Defining the following small amplitude perturbations form for $\overline{h}_r, \Delta\overline{h}$ and $\overline{Q}_r$ as follows

$$\begin{cases} \overline{h}_r = \overline{h}_{r0} + \varepsilon_1^*e^{i\tau}\cos\theta_r + \varepsilon_0\varphi_1^*e^{i\tau}\sin\theta_r \\ \Delta\overline{h} = \Delta\overline{h}_0 + \varepsilon_1e^{i\tau}\Delta\overline{h}_1 + \varepsilon_0\varphi_1e^{i\tau}\Delta\overline{h}_2 \\ \overline{Q}_r = \overline{Q}_{r0} + \varepsilon_1e^{i\tau}\overline{Q}_{r1} + \varepsilon_0\varphi_1e^{i\tau}\overline{Q}_{r2} \end{cases} \tag{13}$$

where, $\left.\overline{Q}_{r1} = \dfrac{\partial\overline{Q}_r}{\partial\varepsilon}\right|_{\varepsilon=\varepsilon_0}$; $\left.\overline{Q}_{r2} = \dfrac{1}{\varepsilon_0}\dfrac{\partial\overline{Q}_r}{\partial\varphi}\right|_{\varphi=\varphi_0}$

Substituting Eq. (12-13) in Eq. (7), and collecting the similar linear terms, results the three following equations

$$\overline{q}_{s0} = \delta_c(\boldsymbol{1}_{4x1} - \overline{p}_{r0}) = \overline{Q}_{r0}\overline{p}_{r0} + \Phi\Delta\overline{h}_0 \tag{14}$$

$$(\overline{Q}_{r0} + \delta_c\boldsymbol{I}_{4x4} + i\Pi\overline{V}_e)\overline{p}_{r1} = -\overline{Q}_{r1}\overline{p}_{r0} - \Phi\Delta\overline{h}_1 - i\Theta\cos\theta_r + \overline{g}_{s1} \tag{15}$$

$$(\overline{Q}_{r0} + \delta_c\boldsymbol{I}_{4x4} + i\Pi\overline{V}_e)\overline{p}_{r2} = -\overline{Q}_{r2}\overline{p}_{r2} - \Phi\Delta\overline{h}_2 - i\Theta\cos\theta_r + \overline{g}_{s2} \tag{16}$$

The steady state recess pressure vector $\overline{p}_{r0}$ is obtained solving Eq. (14), and the dynamic recess pressures $\overline{p}_{r1}$ and $\overline{p}_{r2}$ vectors are obtained by solving Eq. (15) and Eq. (16), respectively.

2.2. AHJB Dynamic Coefficients

The stiffness and damping coefficients of the AHJB are determined by considering the dynamic restoring forces due to small amplitude perturbed film pressure $\varepsilon_1^*e^{i\omega t}P_1$ and $\varepsilon_0\varphi_1^*e^{i\omega t}P_2$ around the steady state journal equilibrium position, as presented by Ghosh *et al.* (1989). Considering the perturbed film pressure $\varepsilon_1^*e^{i\omega t}P_1$, the restoring forces along ε_0 and φ_0 directions, denoted by $W_{1\varepsilon}$ and $W_{1\varphi}$, respectively, also can be written as a function of linearized stiffness and damping coefficients. Defining the dimensionless force $\overline{W}_1 = W_1/LDP_{s0}\varepsilon_1^*$ and the perturbation frequency ratio $\overline{\omega}=\omega/\Omega$, the following dimensionless stiffness ($\overline{K}_{\varepsilon\varepsilon}$, $\overline{K}_{\varphi\varepsilon}$) and damping ($\overline{B}_{\varepsilon\varepsilon}$, $\overline{B}_{\varphi\varepsilon}$) coefficients can be deduced

$$\begin{cases} \overline{K}_{\varepsilon\varepsilon} = -\,Re\{\overline{W}_{1\varepsilon}\} = \dfrac{K_{\varepsilon\varepsilon}c}{LDP_{s0}} & \overline{K}_{\varphi\varepsilon} = -\,Re\{\overline{W}_{1\varphi}\} = \dfrac{K_{\varphi\varepsilon}c}{LDP_{s0}} \\ \overline{B}_{\varepsilon\varepsilon} = -\dfrac{Im\{\overline{W}_{1\varepsilon}\}}{\overline{\omega}} = \dfrac{B_{\varepsilon\varepsilon}c\Omega}{LDP_{s0}} & \overline{B}_{\varphi\varepsilon} = -\dfrac{Im\{\overline{W}_{1\varphi}\}}{\overline{\omega}} = \dfrac{B_{\varphi\varepsilon}c\Omega}{LDP_{s0}} \end{cases} \tag{17}$$

Similarly, considering the perturbed film pressure $\varepsilon_0\varphi_1^*e^{i\omega t}P_2$, the restoring forces along ε_0 and φ_0 directions, denoted by $W_{2\varepsilon}$ and $W_{2\varphi}$, respectively, the others resultant stiffness ($\overline{K}_{\varphi\varphi}$, $\overline{K}_{\varepsilon\varphi}$) and damping ($\overline{B}_{\varphi\varphi}$, $\overline{B}_{\varepsilon\varphi}$) coefficients, by using the dimensionless force $\overline{W}_2 = W_2/LDP_{s0}\varepsilon_0\varphi_1^*$, are given as follows

$$\begin{cases} \overline{K}_{\varepsilon\varphi} = -\,Re\{\overline{W}_{2\varepsilon}\} = \dfrac{K_{\varepsilon\varphi}c}{LDP_{s0}} & \overline{K}_{\varphi\varphi} = -\,Re\{\overline{W}_{2\varphi}\} = \dfrac{K_{\varphi\varphi}c}{LDP_{s0}} \\ \overline{B}_{\varepsilon\varphi} = -\dfrac{Im\{\overline{W}_{2\varepsilon}\}}{\overline{\omega}} = \dfrac{B_{\varepsilon\varphi}c\Omega}{LDP_{s0}} & \overline{B}_{\varphi\varphi} = -\dfrac{Im\{\overline{W}_{2\varphi}\}}{\overline{\omega}} = \dfrac{B_{\varphi\varphi}c\Omega}{LDP_{s0}} \end{cases} \tag{18}$$

The bearing stiffness and damping coefficients may be used in rotor dynamic calculations for unbalance and random vibration responses, for determining damped critical speeds and for rotor stability analysis. For these purposes,

representing the bearing dynamic coefficients in the *XY* inertial coordinate system is more suitable than in εφ reference system. Equation (19) provides the dynamic coefficients conversion between these two reference coordinate systems.

$$\begin{bmatrix} \overline{K}_{XX} & \overline{K}_{XY} \\ \overline{K}_{YX} & \overline{K}_{YY} \end{bmatrix} = \boldsymbol{T}' \begin{bmatrix} \overline{K}_{\varepsilon\varepsilon} & \overline{K}_{\varepsilon\varphi} \\ \overline{K}_{\varphi\varepsilon} & \overline{K}_{\varphi\varphi} \end{bmatrix} \boldsymbol{T} \quad \text{and} \quad \begin{bmatrix} \overline{B}_{XX} & \overline{B}_{XY} \\ \overline{B}_{YX} & \overline{B}_{YY} \end{bmatrix} = \boldsymbol{T}' \begin{bmatrix} \overline{B}_{\varepsilon\varepsilon} & \overline{B}_{\varepsilon\varphi} \\ \overline{B}_{\varphi\varepsilon} & \overline{B}_{\varphi\varphi} \end{bmatrix} \boldsymbol{T} \tag{19}$$

where, $\boldsymbol{T} = \begin{bmatrix} cos\,\varphi_0 & sin\,\varphi_0 \\ -sin\,\varphi_0 & cos\,\varphi_0 \end{bmatrix}$ is the coordinate transformation matrix.

3. Numerical Analysis and Results

The HJB static and dynamic characteristics were extensively investigated by considering different design and operational parameters, characterized by the Sommerfeld number (Watanabe, 2003). Figure 2 shows an example of the journal bearing static dimensionless pressure $\overline{P}_0$ distribution on the land surfaces and recesses. The static dimensionless pressures $\overline{P}_{r0}^{(n)}$ in the recesses *1,2,3* and *4* are: *0.275*, *0.388*, *0.856* and *0.416*, respectively.
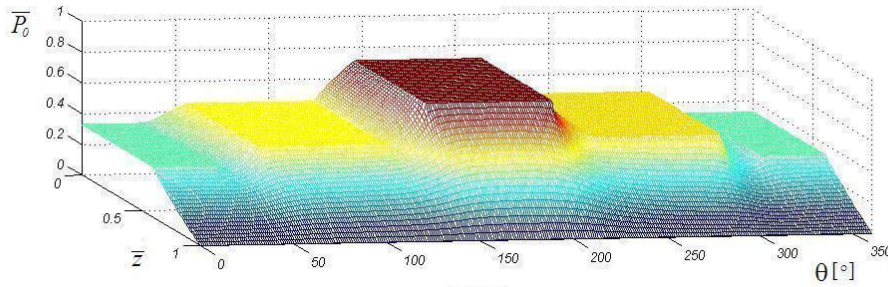
Figure 2. HJB dimensionless static pressure $\overline{P}_0$ distribution, for *L/D=1*, *a=L/5*, *b=πD/16*, ε_0=0.5 and Λ=2

The feasibility of influencing the AHJB dynamic fluid film coefficients by the feedback control system gains, aiming the rotor-bearing systems stabilization and vibration reduction was investigated (Santos and Watanabe, 2003). The compensation of the cross-coupling stiffness coefficients and the increase of the direct damping coefficients, leading to rotor-bearing systems with larger threshold of stability were proposed, and the influence of the feedback control gains in the bearing dynamic coefficients were investigated, considering a fixed rotation and a synchronous perturbation frequency, due to rotor unbalance. Assuming that, $g_1 = g_{1X} = g_{1Y}$ and $g_2 = g_{2X} = g_{2Y}$, and individually varying the k_g, g_1 and g_2 gains, it was observed that due to servovalve working limitations, it is not recommended the retrofit the velocity signals (Santos and Watanabe, 2004).

The feasibility of applying a HJB in a industrial gas compressor, with and without active lubrication, was analyzed by the authors, aiming the reduction of the rotor unbalance response in critical speeds to safety operation conditions. The rotor compressor employed in this analysis is composed of five impellers, weights *391kg*, operates in the range of *6942rpm* (*115.7Hz*) to *10,170rpm* (*169.7Hz*) and is originally supported by tilting-pad bearings and squeeze-film dampers. Santos *et al*. (2003), theoretically investigated the feasibility of applying active lubricated tilting-pad journal bearings in this compressor.

By applying the shaft and disk *finite elements modeling technique* proposed by Nelson and McVaugh (1976), the compressor shaft is modeled with *56* shaft elements and *57* nodes, as illustrated in Fig. 3. Impellers and other machine elements attached to the shaft are considered as rigid discs, whose dynamics are incorporated into the model by adding inertia to respective nodes. Hence, in the model, the impeller are at nodes *20, 24, 28, 32* and *36*; bushes are at nodes *22, 26, 30* and *34*; a thrust disc sleeve is located at node *3*; a balance piston is located at node *38*; seal bushes are located are nodes *12* and *46*, and the coupling is at node *55*. The shaft bearings are located at nodes 8 and *50*.
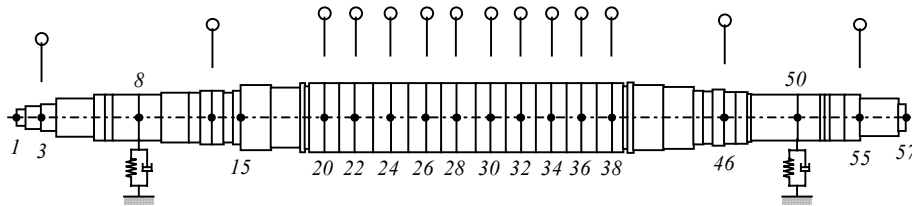
Figure 3. Rotor compressor finite elements model

The bearing and servovalve characteristics adopted in the numerical simulations of the compressor dynamic response are presented in Tab. 1.

Table 1. AHJB geometric and operational characteristics adopted for the rotor-bearing simulations

journal diameter	$D = 100$	mm
bearing width	$L = 45$	mm
circumferential land width	$a = 9$	mm
axial land width	$b = 10$	mm
recess depth	$t_r = 1$	mm
nominal bearing gap	$c = 90$	μm
constant recess supply pressure	$P_{s0} = 1.5$ to 5	MPa
servovalve supply pressure	$P_s = 2P_{s0}$	MPa
lubricant oil dynamic viscosity (*37,8°C*)	$\mu = 0,015$	Ns/m^2
lubricant oil density	$\rho = 900$	kg/m^3
centered recess pressure ratio	$\beta = 0,5$	---
capillary dimensionless parameter	$\delta_c = 17.453$	---
servovalve eigenfrequency	$\omega_v = 2\pi.320$	rad/s
servovalve damping factor	$\zeta_v = 0.55$	---
servovalve gain	$K_v = 1x10^{-5}$	$m^3/s/V$
servovalve linear factor	$K_{PQ} = 1.8x10^{-12}$	$Pa/m^3/s$

As mentioned before, the servovalve input signals U_X and U_Y, resulting from the gain and feedback signals combination, have to be in the range of ±*5%* of the nominal voltage. Besides, bearing dynamic coefficients are only theoretically valid for infinitesimal displacements. However, according to Lund and Thomsen (1978), dynamic coefficients may be used in practical applications for amplitudes up to *50%* of the bearing clearance. Based on these information, the following restrictions of control signal and vibration amplitude were applied to the dynamic coefficients calculations, assuming that the servovalve nominal input signal is ±*10V*, restricting the linear actuating range to ±*0.25V*, and the dynamic displacements amplitudes e^* in *20%* of nominal bearing gap, i.e., *0.2c*

$$\begin{cases} \dfrac{U_X^*}{e^*} = (1+k_g)\sqrt{g_{1X}^2 + \omega^2 g_{2X}^2} \le \dfrac{0,25}{0,2c} \\[3mm] \dfrac{U_Y^*}{e^*} = (1+k_g)\sqrt{g_{1Y}^2 + \omega^2 g_{2Y}^2} \le \dfrac{0,25}{0,2c} \end{cases} \tag{20}$$

Furthermore, assuming that $g_2 = 0$ and $k_g = 2$, the dynamic coefficients of the AHJB were determined as a function of the g_1 gain and the rotation frequency f_r for different values of supply pressure P_{s0}. Figure 4 and Fig. 5 illustrate, respectively, the stiffness and damping coefficients behavior of the AHJB, for $P_{s0} = 1.5MPa$ (*15bar*).
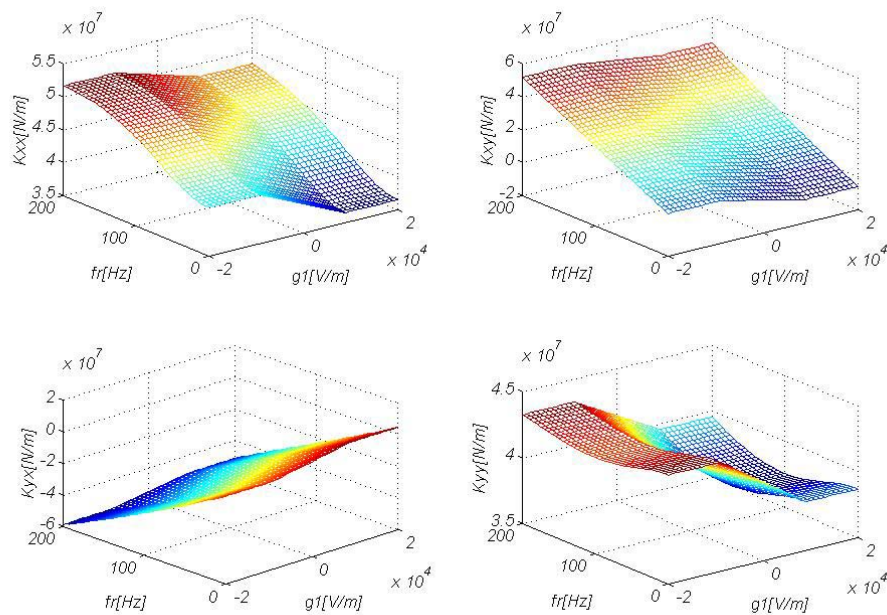
Figure 4. Bearing stiffness coefficients as function of rotation frequency *fr* and proportional gain g_1, for $P_{s0} = 1.5MPa$ (*15bar*)
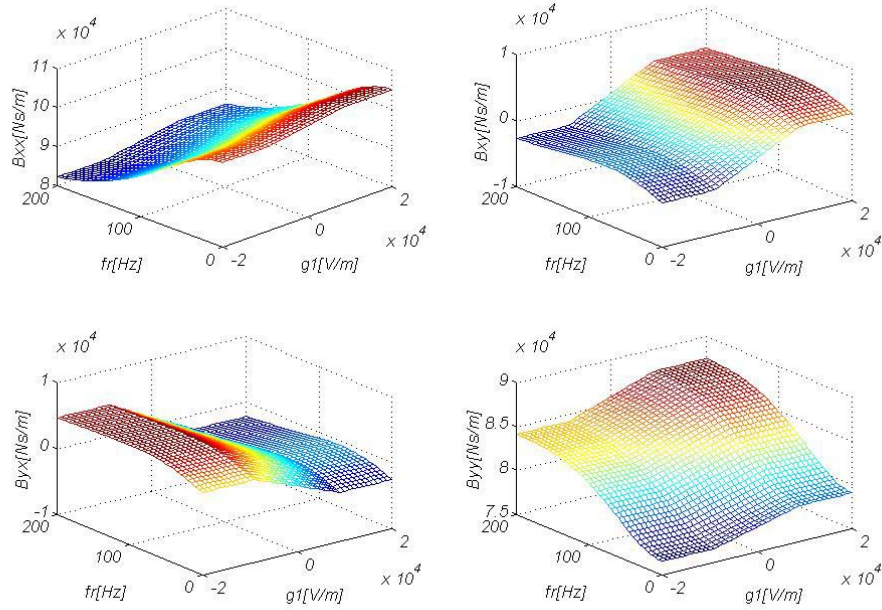
Figure 5. Bearing damping coefficients as function of rotation frequency fr and proportional gain g_1, for $P_{s0}=1.5MPa$ (*15bar*)

One can clearly notice in Fig. 4 and Fig. 5 the influence of rotation frequency and control gain g_1 on the bearing stiffness and damping coefficients. For a given rotation frequency f_r, and varying the control gain g_1, may be noticed three different regions in all figures: two of these regions present constant values of the bearing dynamic coefficients due to servovalve saturation limits.

Bearing dynamic coefficients, like those presented in Fig. 4 and Fig. 5, may be used in the gas compressor finite element model to analyze the rotor dynamic behavior. In this paper, the rotor unbalance response is analyzed by considering the bearing passive lubrication mode (HJB - $g_1=g_2=0$) and the bearing active lubrication mode (AHJB), assuming $g_2=0$, $g_1=9x10^3V/m$ and $k_g=2$. The criteria for choosing a suitable value for control gain g_1 is based on the increasing of damping factor of the first two bending modes of the rotor in *X* and *Y* directions. Applying the criteria established by the norm API 617 (1995), one can analyze the rotor unbalance response. According to this norm, for the case in study, the unbalance value to be applied in the node of maximum displacement of the model is given by $m_u=720g.mm$. According to this same norm, the vibration amplitude limit for the case in study is $L_v=16.65\mu m$.

Results of the rotor unbalance response for the bearing in passive operation are shown in Fig. 6 for different values of P_{s0} and in *X* and *Y* directions. One can notice that, for low values of P_{s0} (*15* or *20bar*), the unbalance responses of the compressor are in accordance with API limit, even in critical speed, but for higher values of P_{s0} (*30, 40* or *50bar*), the unbalance response of the compressor in critical speeds regions are higher them the API limit. The HJB load capacity and stiffness coefficients are strongly influenced by the bearing supply pressure P_{s0}, and for this reason, a suitable choice is necessary to comply with the design requirements and unbalance response limits.
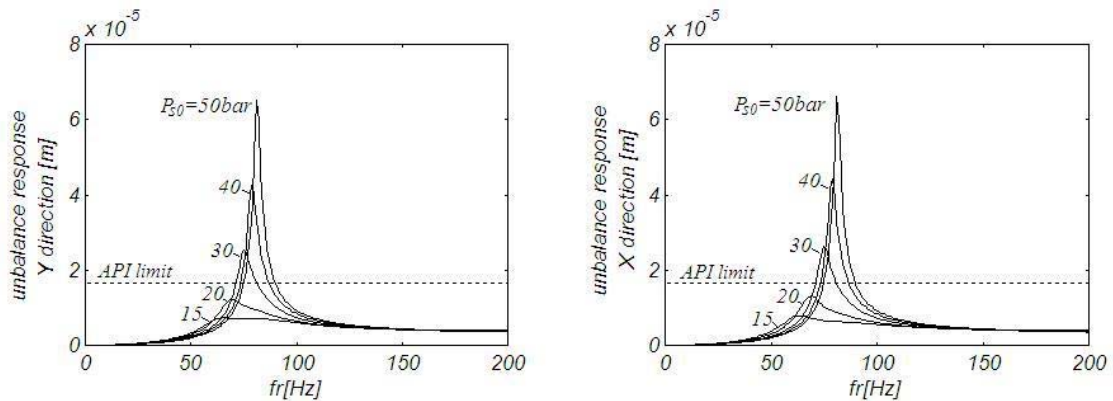
Figure 6. Unbalance response of node *28*, in *Y* and *X* directions, of the compressor supported by HJB

Figure 7 presents the comparison of the passive (HJB) and active (AHJB) lubrication modes in the rotor unbalance response for an intermediate value of the supply pressure P_{s0} (*25bar*), in *X* and *Y* directions, and for both, the API limit

is obeyed only with the active lubrication mode.
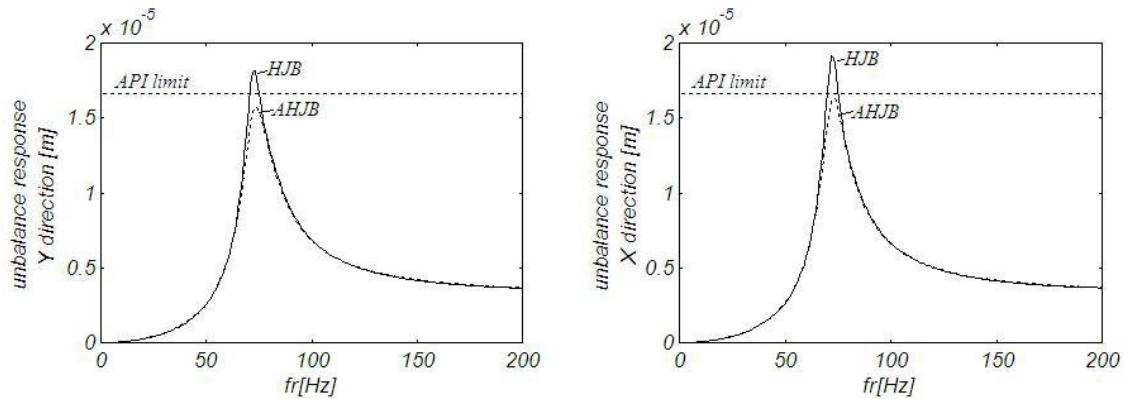
Figure 7. Unbalance response of node *28*, in *Y* and *X* directions, of the compressor supported by HJB and AHJB, for P_{s0}=2.5MPa (*25bar*)

4. Conclusions and Future Aspects

The mathematical modeling technique for calculating the static and dynamic characteristics of hybrid multirecess journal bearings, passively or actively lubricated, was presented. The feasibility of influencing the dynamic fluid film coefficients of the journal bearing by means of the servo control system actuating in fluid injection was theoretically proven, leading to the possibility of investigating different techniques for rotor-bearing systems stabilization and vibration reduction.

The compensation of the cross-coupling stiffness coefficients and the increase of the direct damping coefficients, leading to rotor-bearing systems with larger threshold of stability were proposed, and the influence of the feedback control gains in the bearing dynamic coefficients were investigated, considering a synchronous perturbation frequency. It was observed that, due to servovalve working limitations, the retrofit the velocity signals it is not recommended ($g_2 = 0$), and that the cross-coupling coefficients may only be significantly influenced if a crossed retrofitting control system is adopted ($k_g \neq 0$). The feasibility of applying multirecess journal bearings actively lubricated to an industrial compressor, aiming at reducing lateral vibrations at critical speeds and allowing a wider and safety operation frequency range, is illustrated. Once the stiffness coefficients are strongly influenced by the bearing supply pressure P_{s0}, a suitable choice of the control gains is necessary to comply with the design requirements and unbalance response limits.

A test rig is being built at the Technical University of Denmark for experimental validation of the mathematical model of multirecess journal bearings under active lubrication.

5. References

Althaus, J., Stelter, P. Feldkamp, B. and Adam, H., 1993, "Aktives hydraulisches Lager für eine Schneckenzentrifuge, Schwingungen in rotierenden Machinen II", edited by H. Irretirer, R. Nordmann, H. Springer, Vieweg Verlag, Vol.2, pp.28-36.

API 617 – "Centrifugal Compressors for Petroleum, Chemical, and Gas Service Industries", 1995, 6th ed., American Petroleum Institute.

Bently. D.E., Grant, J.W. and Hanifan, P.C., 2000, "Active Controlled Hydrostatic Bearings for a New Generation of Machines", ASME/IGTI International Gas Turbine & Aeroengine Congress & Exhibition, Munich, Germany, may 8-11, Paper 2000-GT-354.

Edelmann, H., 1986, "Schnelle Proportionalventile und ihre Anwendug, Sonderdruck aus Ölhydraulic und Pneumatik", Vol.30, No.1.

El-Shafei, A. and Hathout, J.P. 1995, "Development and Control of HSFDs for Active Control of Rotor-Bearing Systems", ASME Journal of Eng. for Gas Turbine and Power, Vol.117, No.4, pp.757-766.

Ghosh, M.K., Guha, S.K. and Majumdar, B.C. 1989, "Rotor-Dynamic Coefficients of Multirecess Hybrid Bearings – Part I", Wear, Vol.129, pp.245-259.

Goodwin, M.J., Boroomand, T., and Hooke, C.J. 1989, "Variable Impedance Hydrodynamic Journal Bearings for Controlling Flexible Rotor Vibrations", 12th Biennial ASME Conference on Vibration and Noise, Montreal, Sept.17-21, pp.261-267.

Guha, S.K., Ghosh, M.K. and Majumdar, B.C. 1989, "Rotor-Dynamic Coefficients of Multirecess Hybrid Bearings – Part II: Fluid Inertia Effect", Wear,Vol. 129, pp.261-272.

Lund, J.W. and Thomsen, K.K., 1978, "A Calculation Method and Data for the Dynamic Coefficients of Oil-Lubricated Journal Bearings, in : Topics in Fluid Film Bearing and Rotor Bearing System Design and Opmization", ASME, New York.

Merrit, H. E., 1967, "Hydraulic Control System", John Wiley & Sons.

Neal, T.P. 1974, "Performance Estimation for Electrohydraulic Control Systems", Moog Technical Bulletin 126.

Nelson, H.D. and McVaugh, J. M. 1976, "The Dynamics of Rotor-Bearing Systems Using Finite Element", ASME Journal of Engineering for Industry, Vol.98, No.2, pp.593-600.

Osman, T.A., Nada, G. S. and Safar, Z. S. 2001, "Static and Dynamic Characteristics of Magnetized Journal Bearings Lubricated with Ferrofluid", Tribology International, Vol.34, No.6, pp.369-380.

San Andrés, L. and Lubell, D. 1998, "Imbalance Response of a Test Rotor Supported on Squeeze Film Dampers", ASME Journal of Eng. for Gas Turbines an Power, Vol.120, No.2, pp.397-404.

Santos, I.F., 1994, "Design and Evaluation of Two Types of Active Tilting-Pad Journal Bearings", IUTAM Symposium on Active Control of Vibration, Bath, England, pp.79-87.

Santos, I.F. 1995, "On the Adjusting of the Dynamic Coefficients of Tilting-Pad Journal Bearings", STLE Tribology Transactions, Vol.38, No.3, pp.700-706.

Santos, I.F. and Nicoletti, R. 1999, "THD Analysis in Tilting-Pad Journal Bearings using Multiple Orifice Hybrid Lubrication, ASME Journal of Tribology, Vol.121, No.4, pp.892-900.

Santos, I.F. and Nicoletti, R. 2001, "Influence of Orifice Distribution on Thermal and Static Properties of Hybridly Lubricated Bearings", International Journal of Solids and Structures, Vol.38, No.10-13, pp.2069-2081.

Santos, I.F., Nicoletti, R. and Scalabrin, A. 2003, "Feasibility of Applying Active Lubrication to Reduce Vibration in Industrial Compressors", Proceedings of ASME Turbo Expo 2003 – Land, Sea an Air, Atlanta, June 16-19, 9p.

Santos, I.F. and Russo, F.H. 1998, "Tilting-Pad Journal Bearings with Electronic Radial Oil Injection", ASME Journal of Tribology, Vol.120, No.3, pp.583-594.

Santos, I.F., and Scalabrin, A. 2000, "Control System Design for Active Lubrication with Theoretical and Experimental Examples", ASME/IGTI International Gas Turbine & Aeroengine Congress & Exhibition, Munich, Germany, may 8-11, Paper 2000-GT-643.

Santos, I.F., Scalabrin, A. and Nicoletti, R. 2001, "Ein Beitrag zur aktiven Schmierungstheorie, Schwingungen in Rotierrenden Machinen VI", edited by H. Irretier, R. Nordmann, H. Springer, Vieweg Verlag, Vol.5, pp.21-30.

Santos, I.F. and Watanabe, F.Y., 2003, "Feasibility of Influencing the Dynamic Fluid Film Coefficients of a Multirecess Journal Bearing by Means of Active Hybrid Lubrication", RBCM – Journal of the Brazilian Society of Mechanical Sciences, Vol. 25, No. 2, pp. 154-163.

Santos, I.F. and Watanabe, F.Y., 2004, "Compensation of Cross-Coupling Stiffness and Increase of Direct Damping in Multirecess Journal Bearings using Active Hybrid Lubrication – Part I: Theory", ASME Journal of Trybology, Vol. 126, pp. 146-155.

Ulbrich, H. and Althaus, J. 1989, "Actuator Design for Rotor Control", 12th Biennial ASME Conference on Vibration and Noise, Montreal, Sept.17-21, pp.17-22.

Vance, J.M. and Li, J. 1996, "Test Results of a New Damper Seal for Vibration Reduction in Turbomachinery", ASME Journal of Engineering for Gas Turbines and Power, Vol.118, No.4, pp.843-846.

Watanabe, F.Y., 2003, "Active Lubrication Applyied to Hybrid Journal Bearings", PhD Thesis, Unicamp, 169p. (in portuguese).

6. Responsibility notice

The authors are the only responsible for the printed material included in this paper.